

Structure and Evolution of Stars

Helio and Asteroseismology

Allan Sacha Brun

*CEA Paris-Saclay, Département d'Astrophysique-AIM
Laboratoire Dynamique des Etoiles, des Exo-planètes et
de leur Environnement*

*Visiting Professor at ISEE, University of Nagoya
(abrun@ihest.science and sacha.brun@cea.fr)*

I am thankful to my colleagues Dr. R. Garcia and Dr. S. Breton for sharing some of the slides used in this lecture

Probing the interior structure and dynamics of Stars

- Several techniques to measure surface rotation
- Only **asteroseismology** for internal rotation

Mode

p

g

Restoring force
compressibility
buoyancy

p and g modes
can mix

In solar-like main-
sequence pulsators

p modes

High-frequency, trapped between
the surface and an inner turning
point

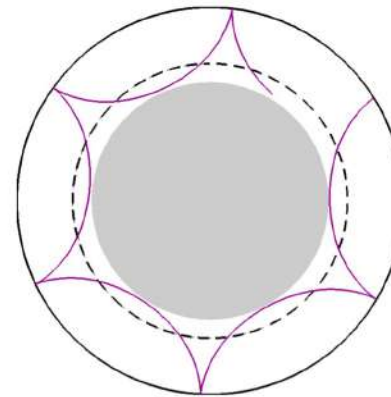
g modes

Low-frequency, trapped inside an
internal resonant stratified cavity
(evanescent in convective zone)

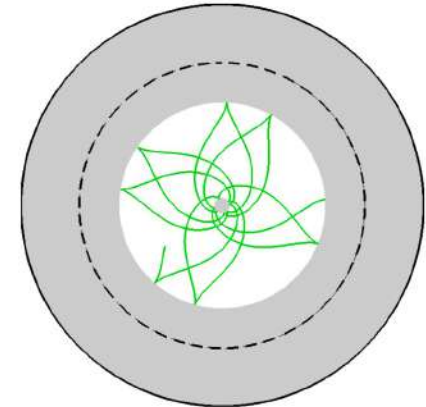
Rotational splittings
+
radial/latitudinal mode
sensitivity

Solar/stellar rotation
profile

p mode



g mode



(adapted from Alvan 2014)

Problem

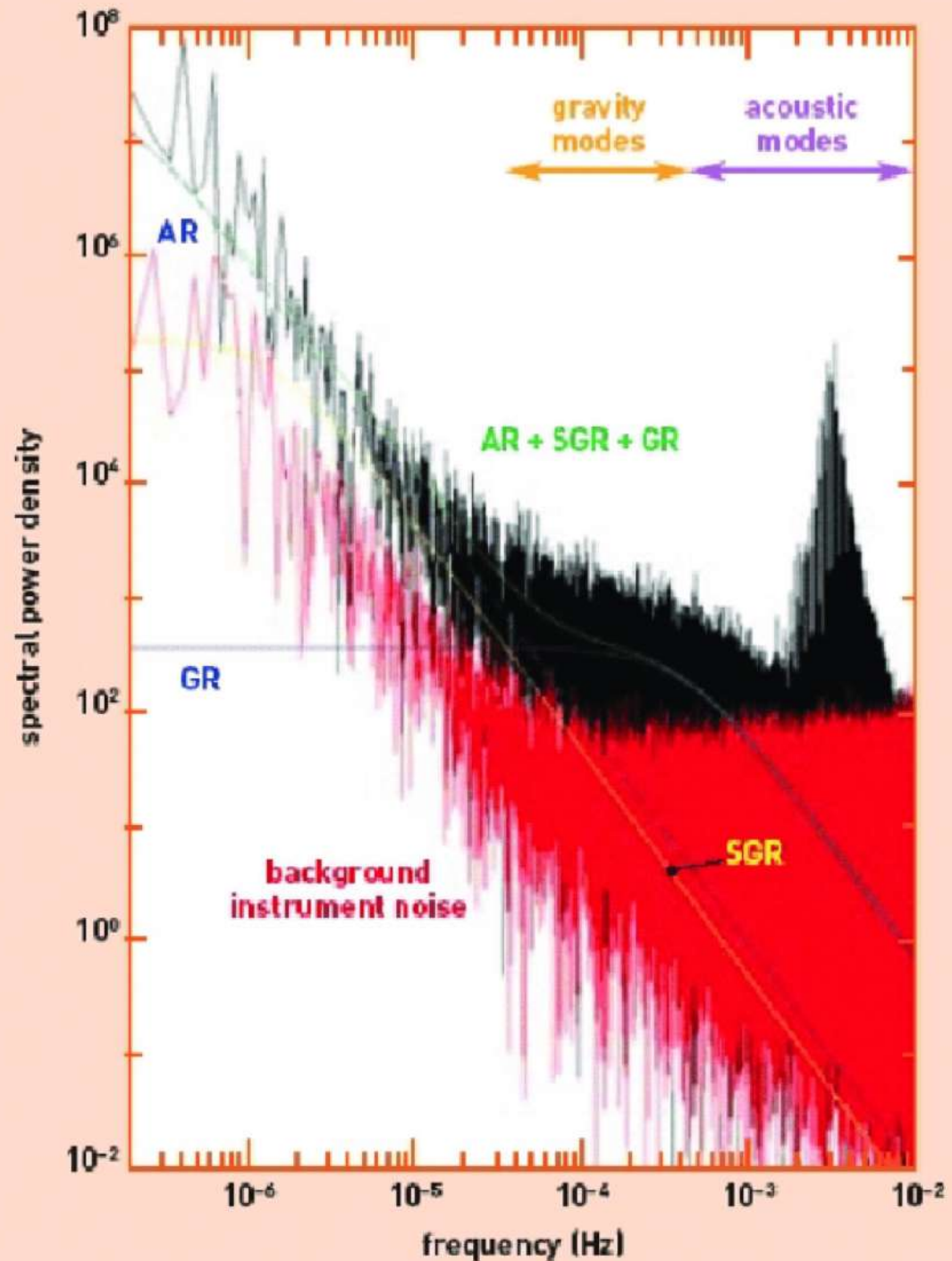
g modes or **mixed modes** are needed to
constrain the rotation profile of inner regions !

Very recent: seismology based on inertial modes in the Sun (Gizon et al. 2021)

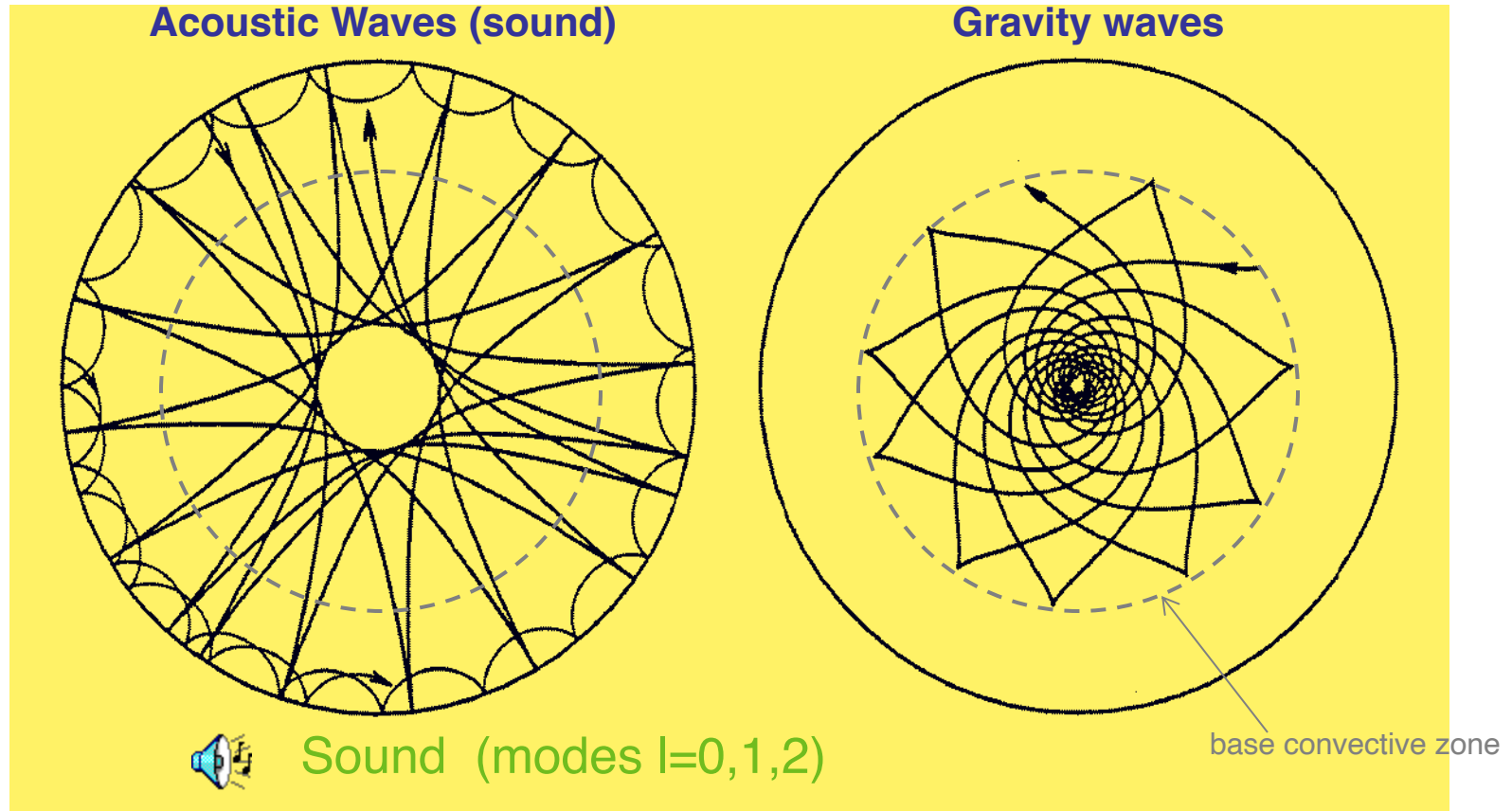
Basics of Helioseismology

Observed solar Acoustic spectra

5 min oscillations



Helioseismology: The Study of Solar Waves



High frequency oscillations
(~ 3 mHz)

Low frequency oscillations
(< 0.4 mHz)

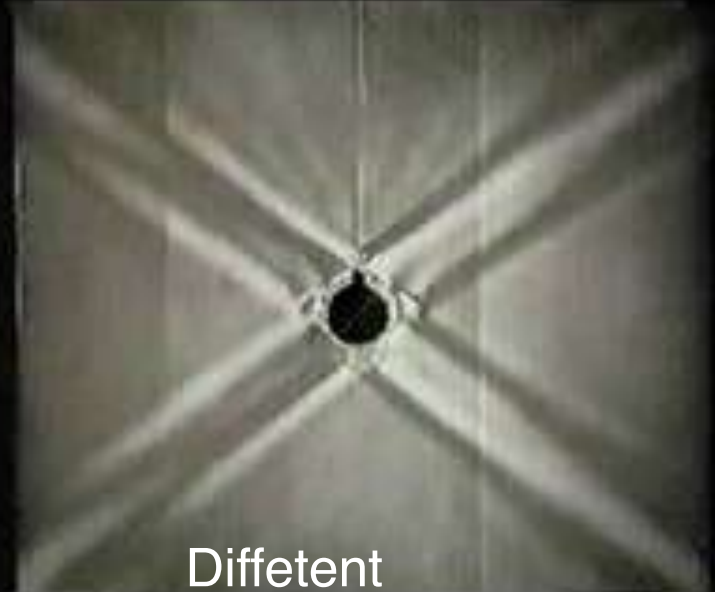
Sound Speed:
500 km/s (core)
200 km/s (base cz)
7 km/s (surface)

The Sun is BIG, it is like a SuperSuper...Bariton

Resonant Modes on a circular plate



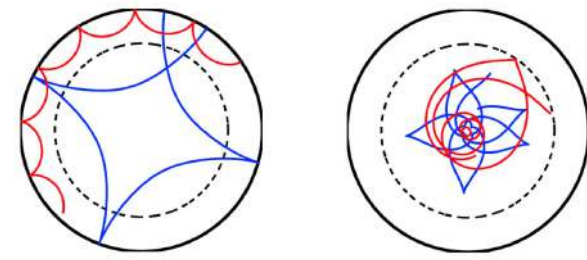
St Andrews Cross Experiment (oscillating rod)



Different frequency leads to different angle of St Andrew cross



Being Seismologists for 1 min



p & g waves



Size



Composition



Dynamic



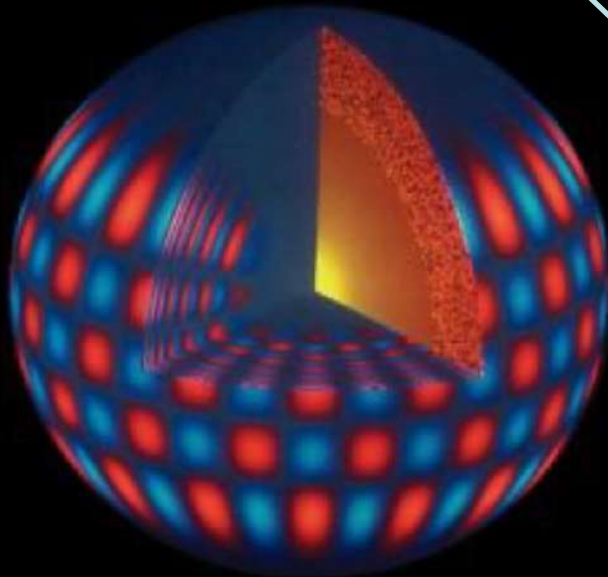
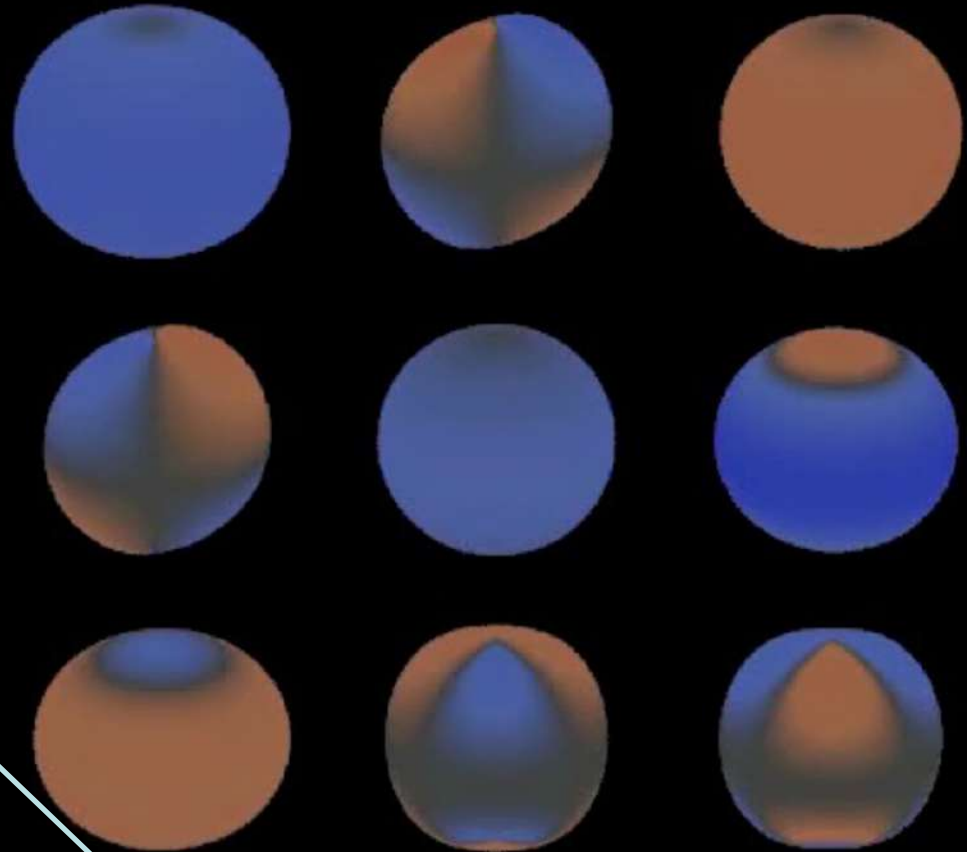
Spherical Harmonics (Y_{lm})

➤ Oscillation eigenmodes:

➤ Characterized by:

- l : Degree
- m : Azimuthal order
- n : Radial Order

A fct of r (n) multiply Y_{lm}
separation of variables
possible under simplifying
hypothesis



▪ Projection on spherical harmonics.

- Each perturbed magnitude f can be expressed:

$$f'(r, \theta, \phi, t) = \sqrt{4\pi} \text{Re} [f'(r) Y_l^m(\theta, \phi) e^{-i\omega_{n,l,m} t}]$$

- Where:

$$Y_l^m(\theta, \phi) = (-1)^m C_{lm} P_l^m(\cos\theta) e^{im\phi}$$

A Reader Digest on Waves inside the Sun

Acoustic and Internal waves are excited inside the Sun

See J. Christensen-Dalsgaard 1997 lecture notes

Wave equation:
$$\frac{d^2 \xi_r}{dr^2} = \frac{\omega^2}{c_s^2} \left(1 - \frac{N^2}{\omega^2} \right) \left(\frac{F_\ell^2}{\omega^2} - 1 \right) \xi_r$$

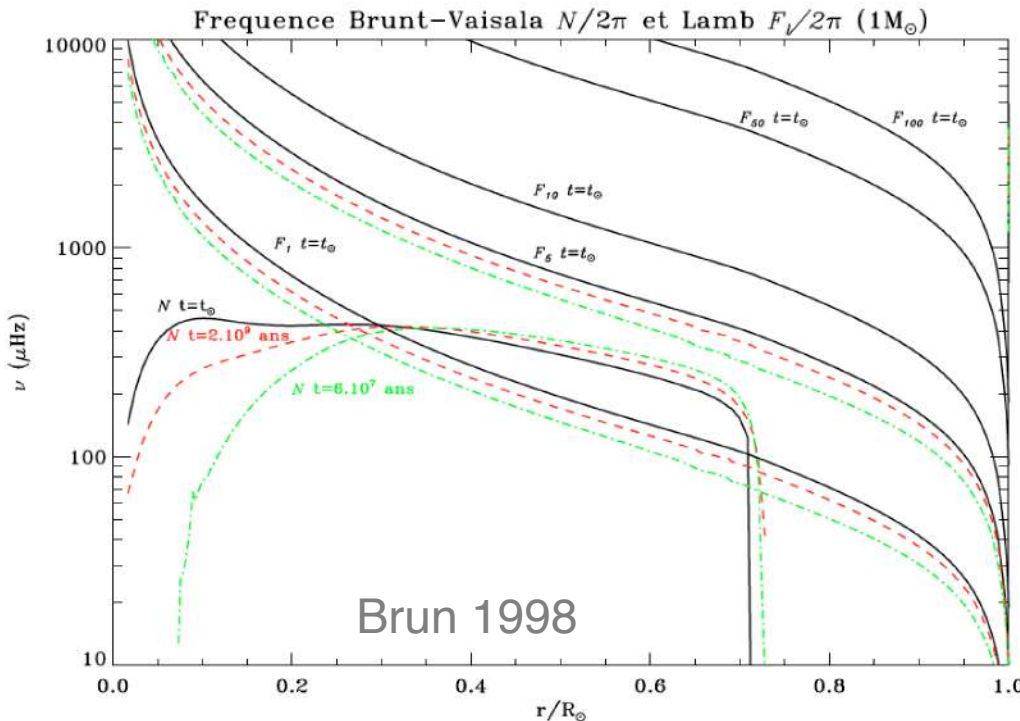
$$N^2 = g_0 \left(\frac{1}{\Gamma_{1,0}} \frac{d \ln p_0}{dr} - \frac{d \ln \rho_0}{dr} \right) \quad F_\ell = S_\ell = l(l+1)c^2/r^2$$

Brunt-Vaisala & Lamb Frequencies – If it's negative, then the solution is oscillatory

- for $|\omega| < |N|$ and $|\omega| < |F_\ell|$,
- or for $|\omega| > |N|$ and $|\omega| > |F_\ell|$.

– if positive, then the solution is exponential

- for $|\omega| < |N|$ and $|\omega| > |F_\ell|$,
- or for $|\omega| < |F_\ell|$ and $|\omega| > |N|$.



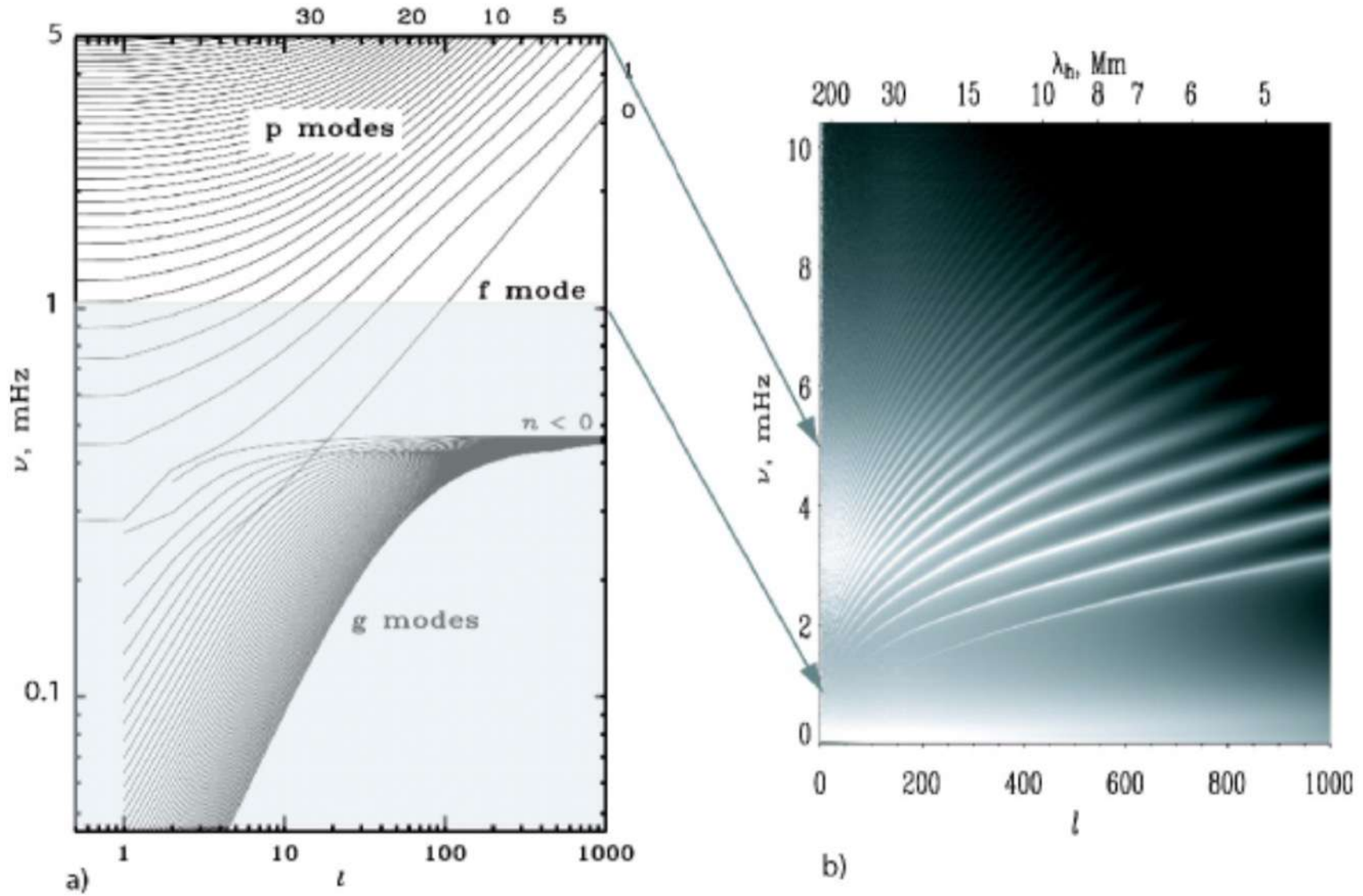
Adding atmosphere cut-off frequency

$$\frac{d^2 X}{dr^2} + \frac{1}{c^2} \left[S_\ell^2 \left(\frac{N^2}{\omega^2} - 1 \right) + \omega^2 - \omega_c^2 \right] X = 0$$

$$\omega_{l,\pm}^2 = \frac{1}{2} [(\omega_c^2 + F_l^2) \pm \sqrt{(\omega_c^2 + F_l^2)^2 - 4F_l^2 N^2}]$$

$$\omega_{\text{cut-off}}^2 = \frac{c_s^2}{4H_\rho^2} \left(1 - 2 \frac{dH_\rho}{dr} \right), \text{ with } H_\rho^{-1} = - \frac{d \ln \rho}{dr}$$

Theoretical and observed solar waves spectra



No clear g-modes detection yet (only possibly their envelope)

Waves Propagation (I)

➤ p modes

- In a solar-like star,

$$\omega \gg N$$

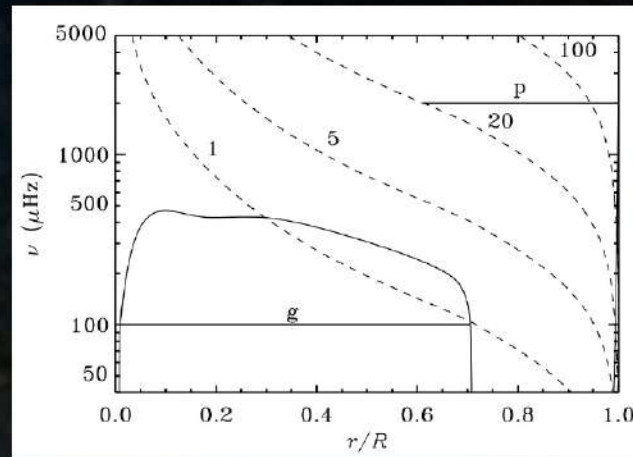
$$K(r) = \frac{\omega^2}{c^2} \left(\frac{N^2}{\omega^2} - 1 \right) \left(\frac{S_l^2}{\omega^2} - 1 \right) \Rightarrow K(r) \simeq \frac{1}{c^2} (\omega^2 - S_l^2)$$

- p modes dynamics => determined only by the variation of the sound speed with r
 - These modes are standing acoustic waves
 - restoring force => dominated by pressure

$$S_l^2 = \frac{l(l+1)c^2}{r^2}$$

➤ Dispersion relation:

- Knowing that $|\mathbf{k}|^2 = k_r^2 + k_h^2$ and $\frac{l(l+1)}{r^2} = k_h^2 \Rightarrow k_r^2 = \frac{1}{c^2} (\omega^2 - S_l^2) \Rightarrow k_r^2 = K$



Asymptotic acoustic (p) modes

- At first order we can obtain (Tassoul 1980):

$$\nu_{nl} = \Delta\nu_0 \left(n + \frac{\ell}{2} + \underbrace{\frac{1}{4} + \alpha(\nu)}_{\varepsilon} \right) + \mathcal{O}\left(\frac{1}{\nu}\right)$$

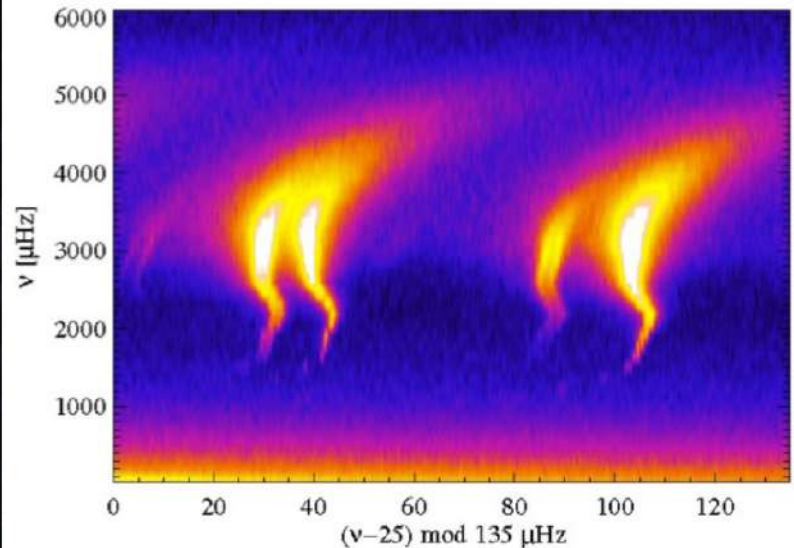
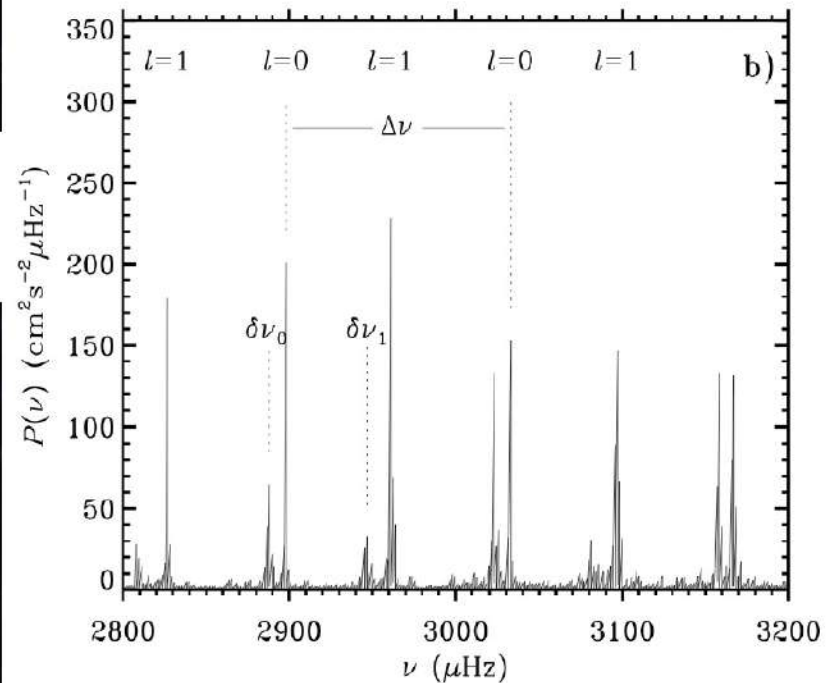
- Combination of frequencies:

- Large separation:

$$\delta_1 \nu_{nl} \equiv \boxed{\Delta\nu_{nl} = \nu_{n+1,l} - \nu_{n,l}} \approx \frac{\partial \nu_{nl}}{\partial n}.$$

- Small separation:

$$\boxed{\delta_{\ell,\ell+2} \nu_{n,l} = \nu_{n,l} - \nu_{n-1,\ell+2}}.$$



Rotation Splitting

Stars rotate, so there is a rotation lift of the degeneracy of the modes $(2\ell+1)$ m 's.

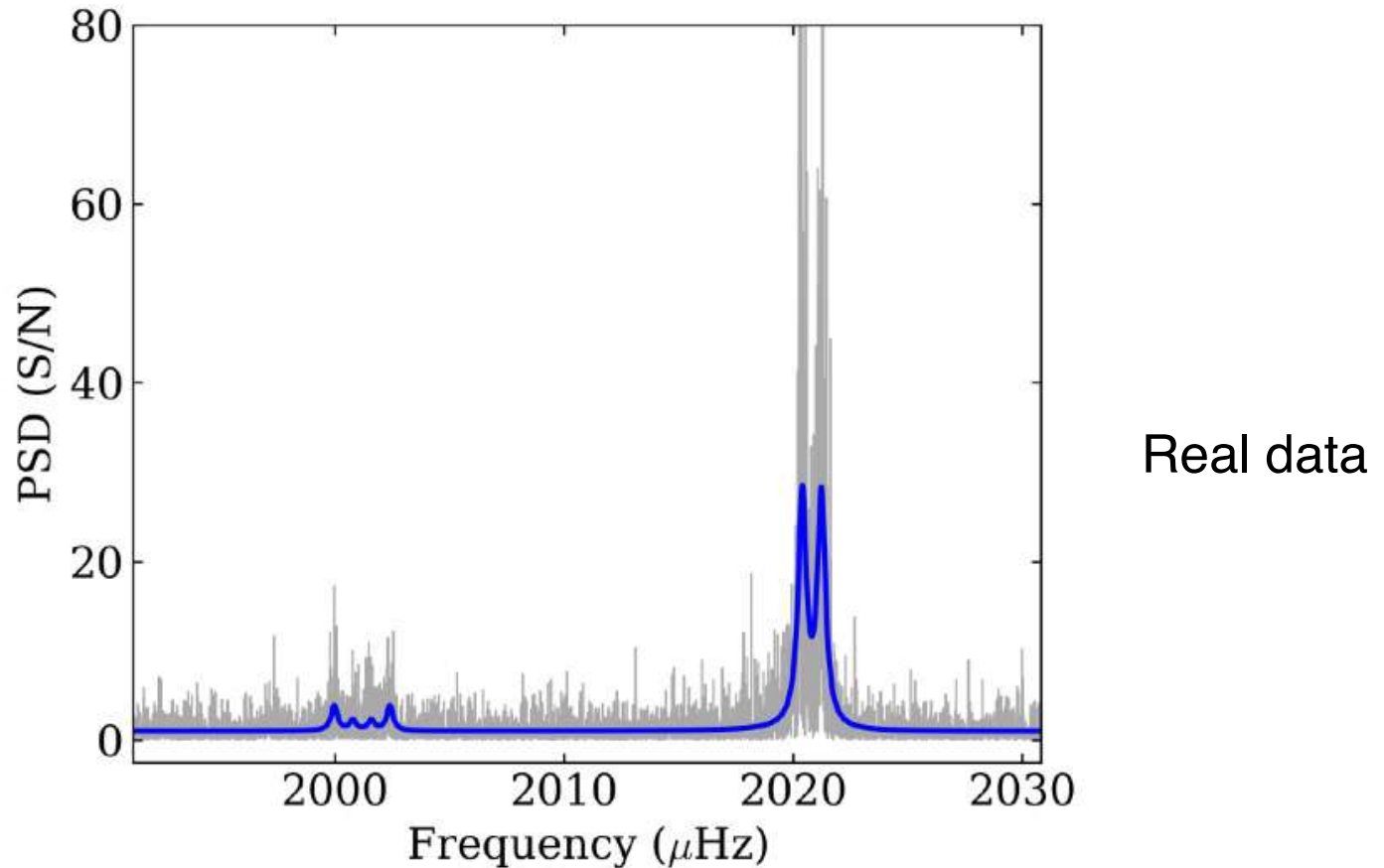
$$\nu_{n,\ell,m} = \nu_{n,\ell} + \delta\nu_{n,\ell,m}.$$

We can get a first idea of what $\delta\nu_{n,\ell,m}$ looks like by using a geometrical argument. Consider for the sake of simplicity, that the angular velocity is constant, e.g. $\Omega(r, \theta) = \Omega_s$, and assume an oscillation with a frequency $\nu_{n,\ell}$, independent of m , in the star's rotating frame R' . One can define a local system of coordinates in R' (r', θ', ϕ') which is related to the inertial frame coordinate system R (r, θ, ϕ) by $(r', \theta', \phi') = (r, \theta, \phi - \Omega_s t)$. Assuming a temporal dependency in $\exp(i\omega_{R'} t)$ in the rotating frame, the real part of the perturbations depends on ϕ' and t as $\cos(m\phi' - \omega_{R'} t)$, hence, the dependence in the inertial frame is $\cos(m\phi - \omega_R t)$, where:

$$\omega_R = \omega_{R'} + m\Omega_s \text{ or } \nu_{n,\ell,m} = \nu_{n,\ell} + m \frac{\Omega_s}{2\pi}.$$

This relation implies that an observer in the inertial frame R sees a frequency shift that depends linearly on m . Such splitting of the mode of degree ℓ in several (i.e. $2\ell+1$) sub-peaks or multiplets²³, is called *rotational splitting* of the modes (Christensen-Dalsgaard 1997). Note that since m take

Rotation Splitting

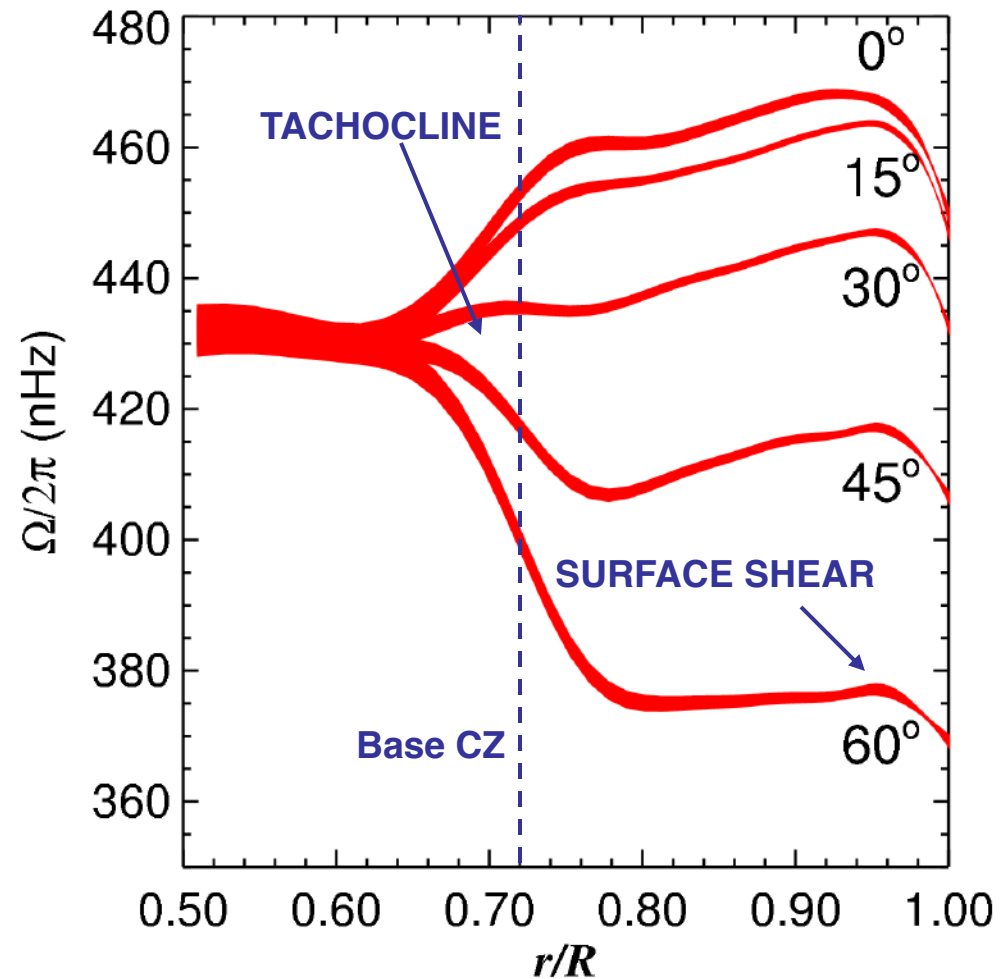
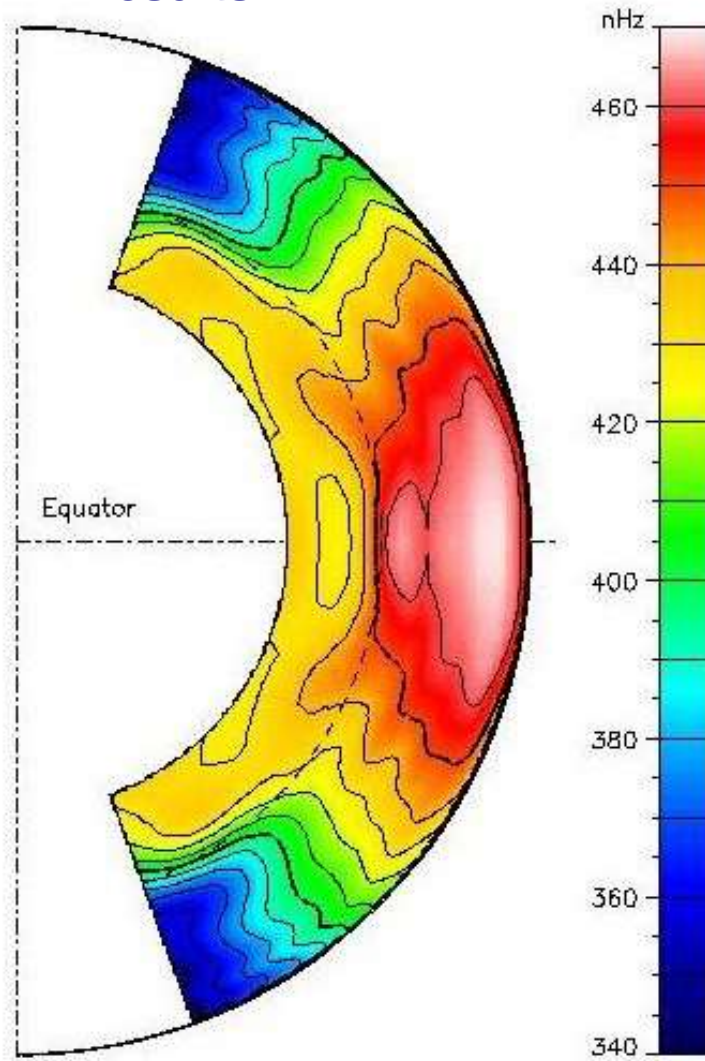


Note that while theoretically the number of multiplets is $2\ell + 1$, observationally it depends on the angle of inclination of the star (Gizon and Solanki, 2003). In the case of the Sun, with a rotational axis perpendicular to Earth's orbital plane, this means that only the even $\ell + m$ modes are seen, so $m = 0$ and $m = 2$ for the multiplets $\ell = 2$ shown in Figure

Solar Internal Rotation

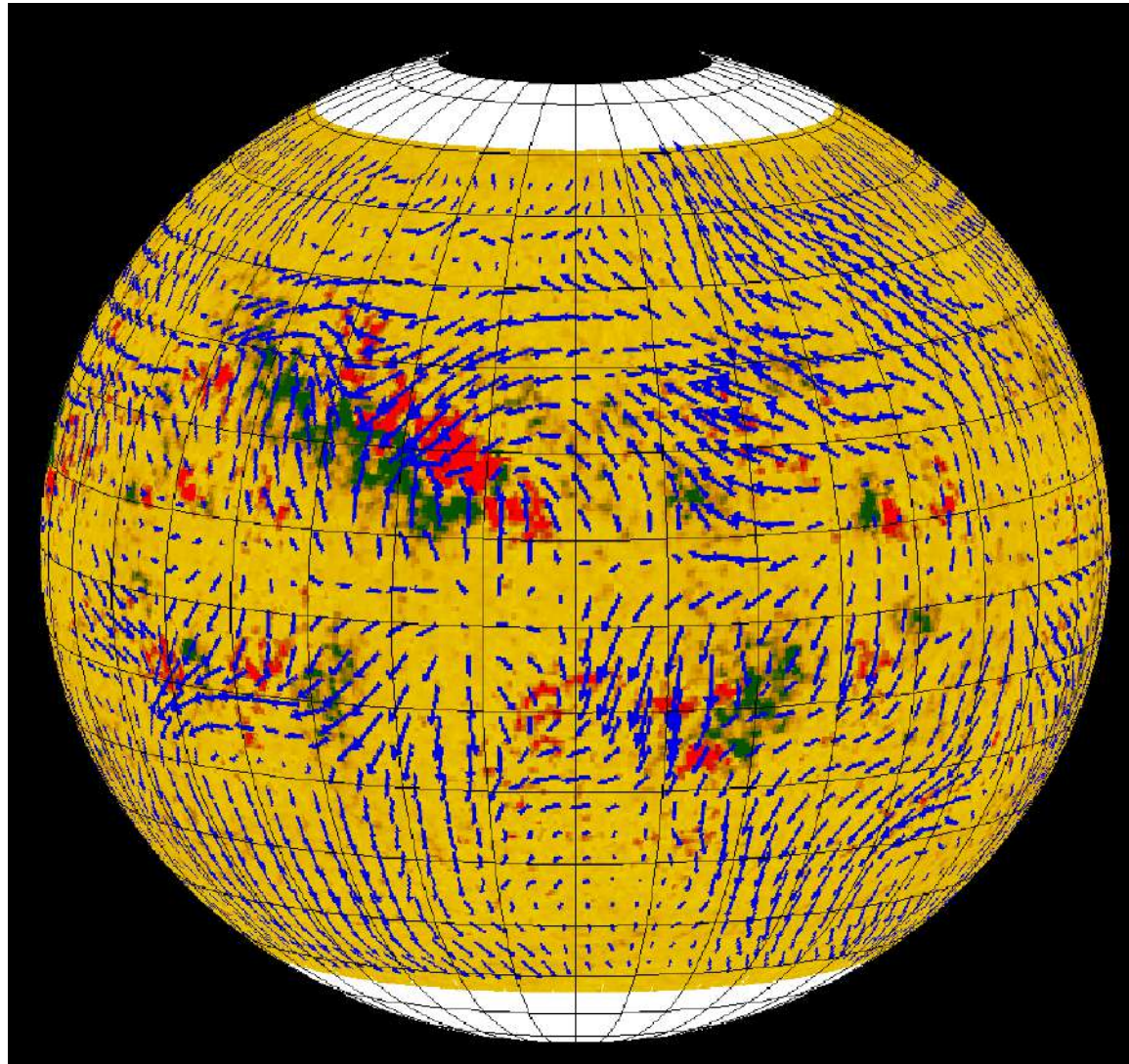
(GONG, MDI data)

Helioseismology Results



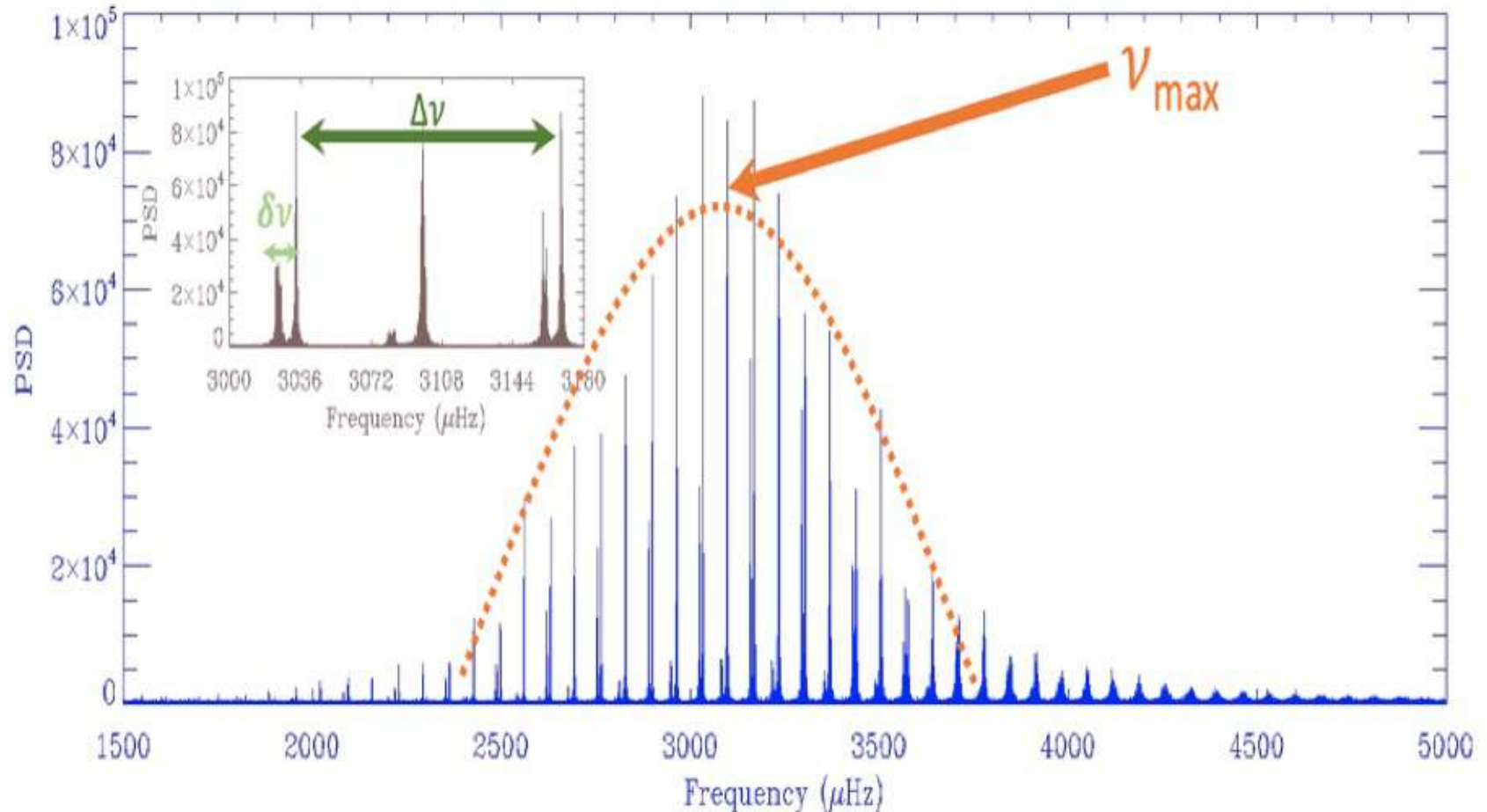
Solar SubSurface Weather

(MDI data)



(Haber et al.
2002)

Large, small frequency differences and ν_{max}



$$\nu_{max} \simeq \nu_{max,\odot} \left(\frac{M_*}{M_\odot} \right) \left(\frac{R_*}{R_\odot} \right)^{-2} \left(\frac{T_{\text{eff}}}{T_{\text{eff},\odot}} \right)^{-1/2}$$

in which $T_{\text{eff},\odot} = 5770 \text{ K}$, and $\nu_{max,\odot} = 3090 \pm 30 \mu\text{Hz}$.

Waves Propagation (II)

➤ g modes

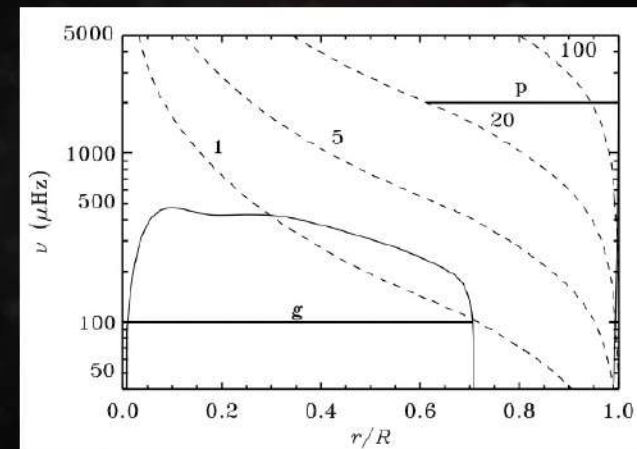
- The turning points are determined by $N = \omega$
- For the Sun =>
 - internal turning point close to the center
 - external turning point at the base of the convective zone
 - For high-order g modes $\omega^2 \ll S_l^2$

$$K(r) = \frac{\omega^2}{c^2} \left(\frac{N^2}{\omega^2} - 1 \right) \left(\frac{S_l^2}{\omega^2} - 1 \right) \quad \Rightarrow \quad K(r) \simeq \frac{1}{\omega^2} (N^2 - \omega^2) \frac{l(l+1)}{r^2}$$

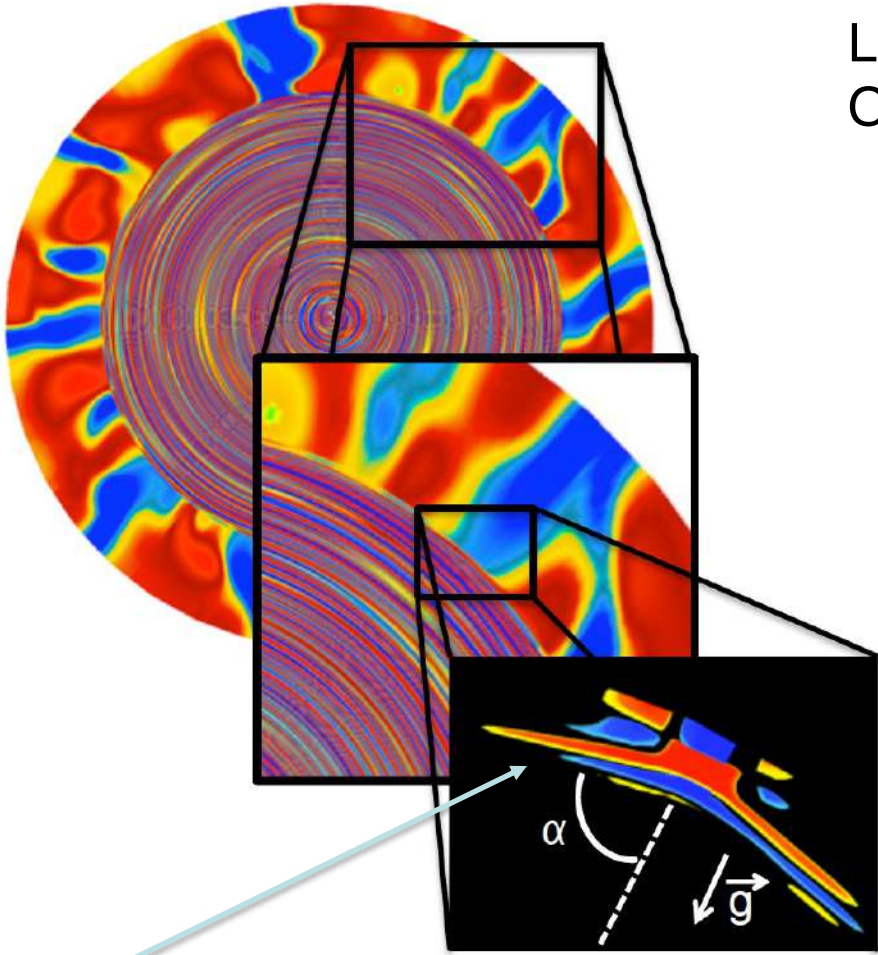
- g modes dynamics => dominated by the variation of the buoyancy frequency N with r
 - These modes are standing gravity waves
 - restoring force => buoyancy

➤ Dispersion relation

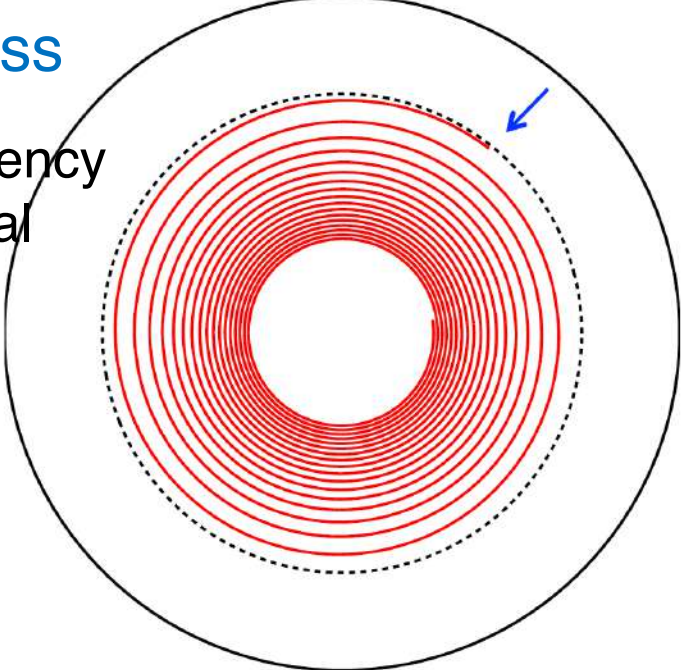
$$k_r^2 = \frac{l(l+1)}{r^2} \left(\frac{N^2}{\omega^2} - 1 \right)$$



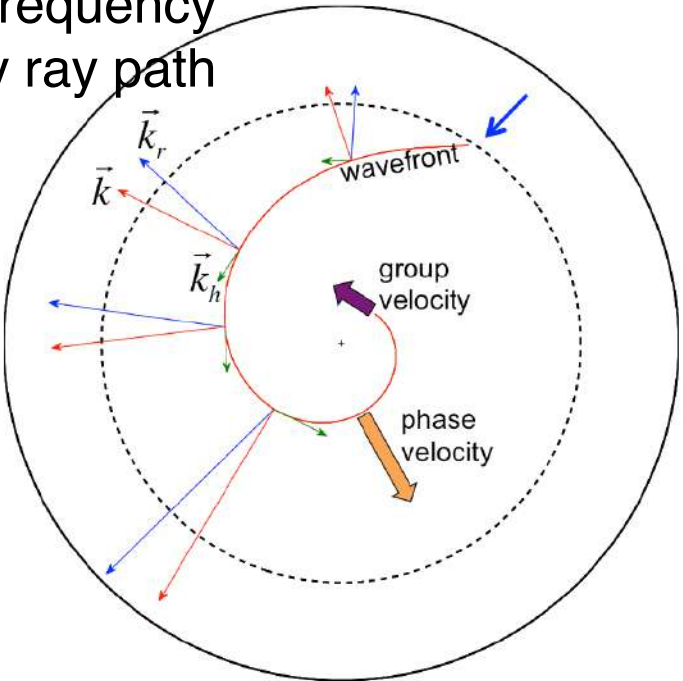
Gravity (internal) waves & St Andrew cross



Low frequency
Open spiral



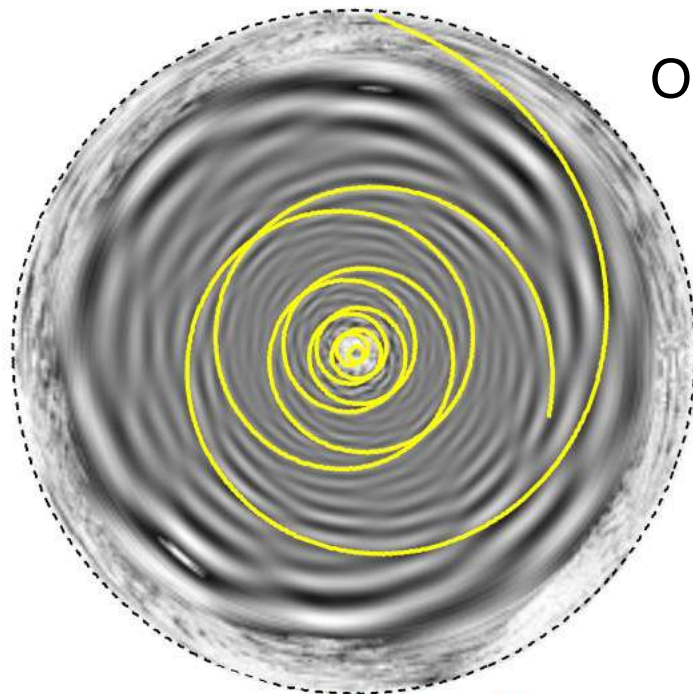
High frequency
Cuspy ray path



St Andrew's cross (Lighthill 1986; Voisin 1991). The wave's energy is radiated around an angle α_{th} to the radial direction such that

$$\alpha_{th} = \arccos\left(\frac{\omega}{N_1}\right),$$

where N_1 is the value of N in the region considered.



Open spiral

$$r_{in} = 0.02 R_{\odot}$$

$$r_{out} = 0.69 R_{\odot}$$

$$\omega = 0.05 \text{ mHz}$$

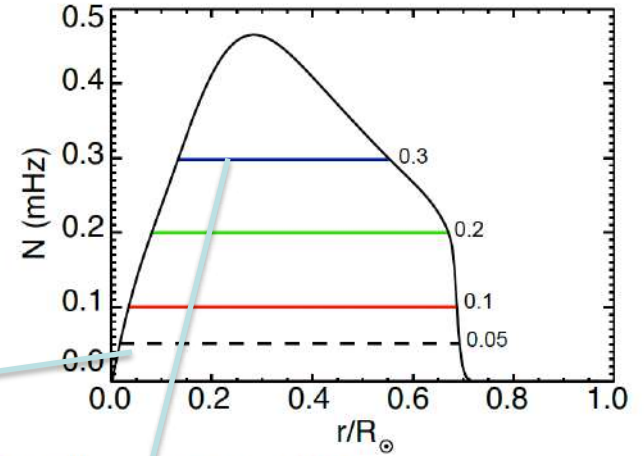
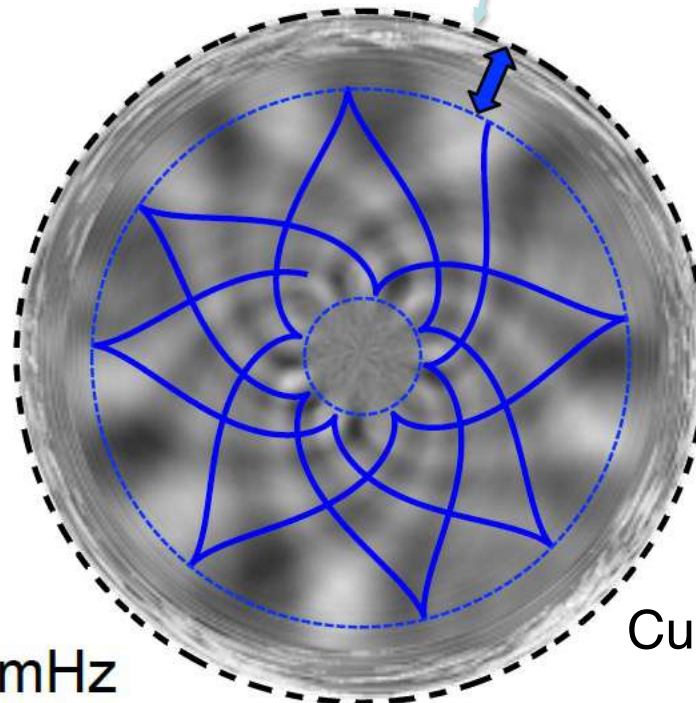


Fig. 1. Profile of the Brunt-Väisälä frequency as a function of the normalized radius. Colored horizontal lines highlight the regions of propagation of the waves revealed by our filtering technique in Fig.

Comparison between ray path (see slide 24) and Fourier transform of 3D ASH simulation. Excellent agreement, note the little viscous spread in Simulation due to limited Re nb.



$$r_{in} = 0.13 R_{\odot}$$

$$r_{out} = 0.55 R_{\odot}$$

Cuspy

Alvan, Brun et al. 2014, 2015 0.3 mHz

Asymtotic gravity (g) modes

➤ Turning point:

- When $\omega = N$

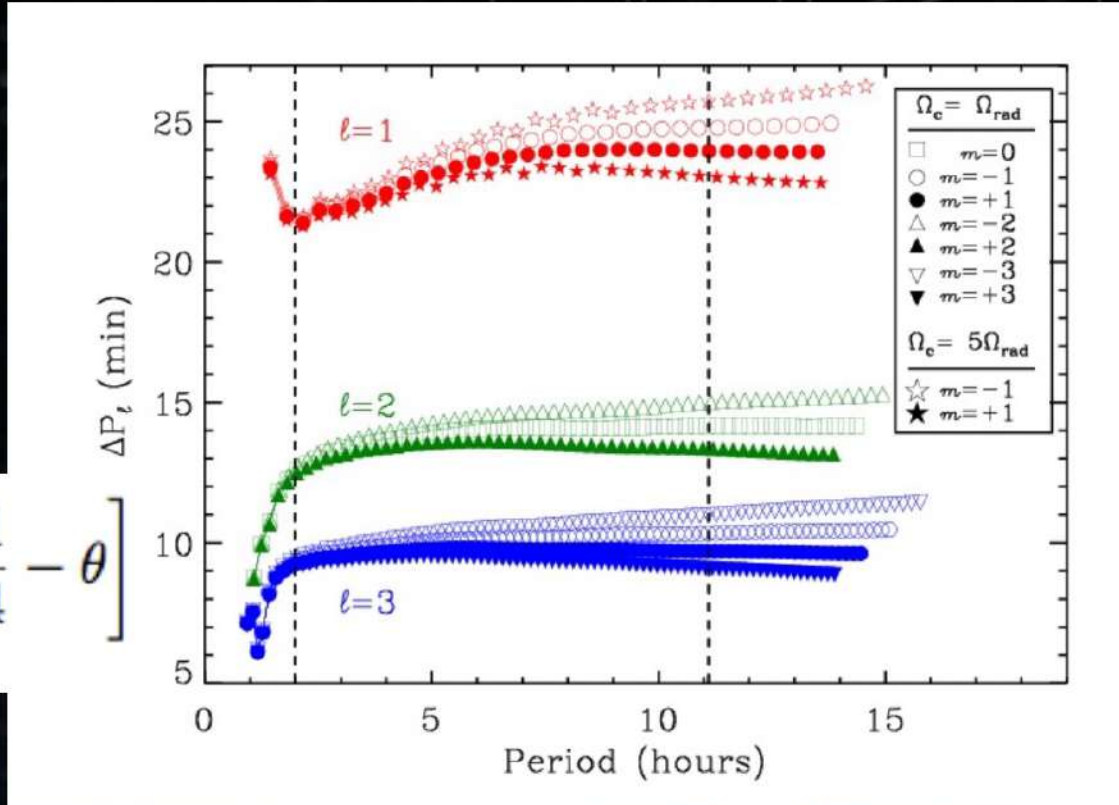
$$\frac{N^2}{\omega^2} - 1 = 0 \quad S_i^2 / \omega^2 \gg 1$$

- At first order (Tassoul 1980)

$$P_{n,l} = \frac{P_o}{\sqrt{l(l+1)}} \left[n + \frac{l}{2} - \frac{1}{4} - \theta \right]$$

$$P_{n,l} = \frac{2\pi}{\omega_{n,l}}$$

$$P_o = 2\pi^2 \left(\int_0^{r_c} \frac{N}{r} dr \right)^{-1}$$



Constant period spacing of g-modes (ASH simulations)

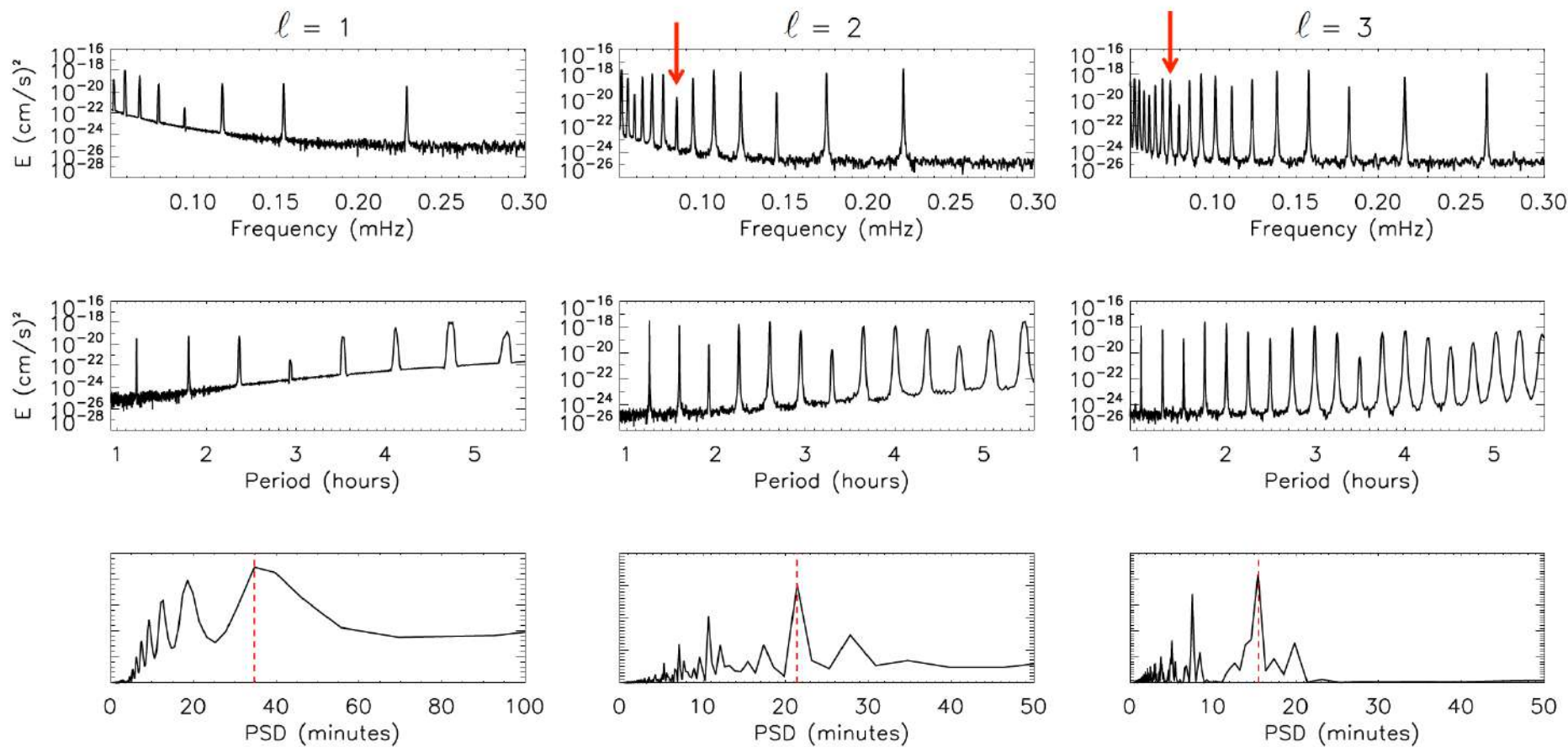
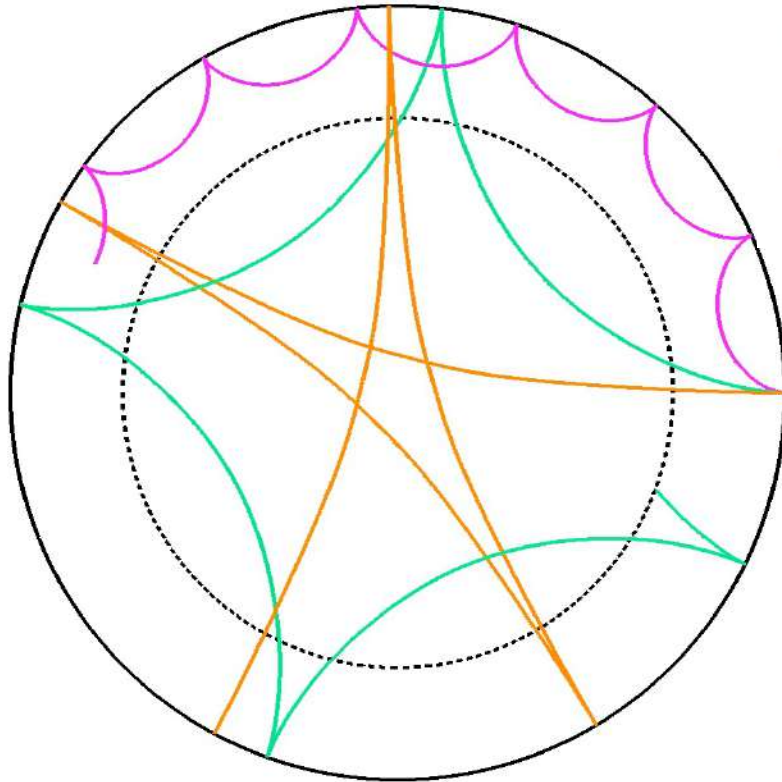


Fig. 17. *Top and middle:* spectrum of gravity waves for $\ell = 1, 2, 3$ as function of frequency and period. *Bottom:* Fourier transform of the middle spectrum that shows the constant period spacing between peaks. We find $\Delta P_1 = 37.1$ min, $\Delta P_2 = 21.2$ min, and $\Delta P_3 = 14.8$ min as pointed out by vertical red dotted lines.

Alvan, Brun et al. 2014, 2015

G vs P-modes: simple ray paths

P-modes

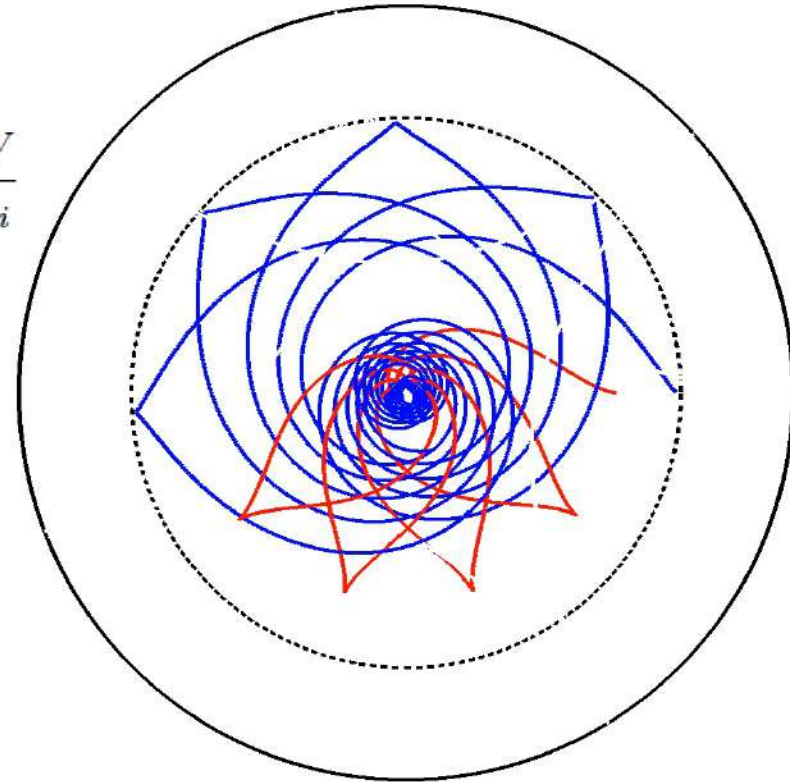


Eikonal Equations

$$\frac{dx_i}{dt} = \frac{\partial W}{\partial k_i}$$

$$\frac{dk_i}{dt} = -\frac{\partial W}{\partial x_i}$$

G-modes



$$k_r^2 = \frac{w^2}{c_s^2} - \frac{l(l+1)}{r^2}$$

$$k_h^2 = \frac{l(l+1)}{r^2}$$

$$w = c_s \sqrt{k_r^2 + k_h^2} = c_s k$$

$$dr = \frac{k_r}{k} c_s dt$$

$$d\theta = \frac{k_h}{k} c_s dt \frac{1}{r}$$

$$k_r^2 = \frac{l(l+1)}{r^2} \left(\frac{N^2}{w^2} - 1 \right)$$

$$k_h^2 = \frac{l(l+1)}{r^2}$$

$$w = \frac{k_h}{\sqrt{k_r^2 + k_h^2}} N = \frac{k_h}{k} N$$

$$dr = -\frac{k_r k_h}{k^2} \frac{N dt}{k}$$

$$d\theta = \left(1 - \frac{k_h^2}{k^2} \right) \frac{N dt}{k} \frac{1}{r}$$

Note: the Eikonal equation allowing to compute the ray paths are indept of l for g-modes, hence changing the order l does not change the ray path (does change the wave speed). Only changing the frequency does.

Recently Discovered Solar Inertial Waves

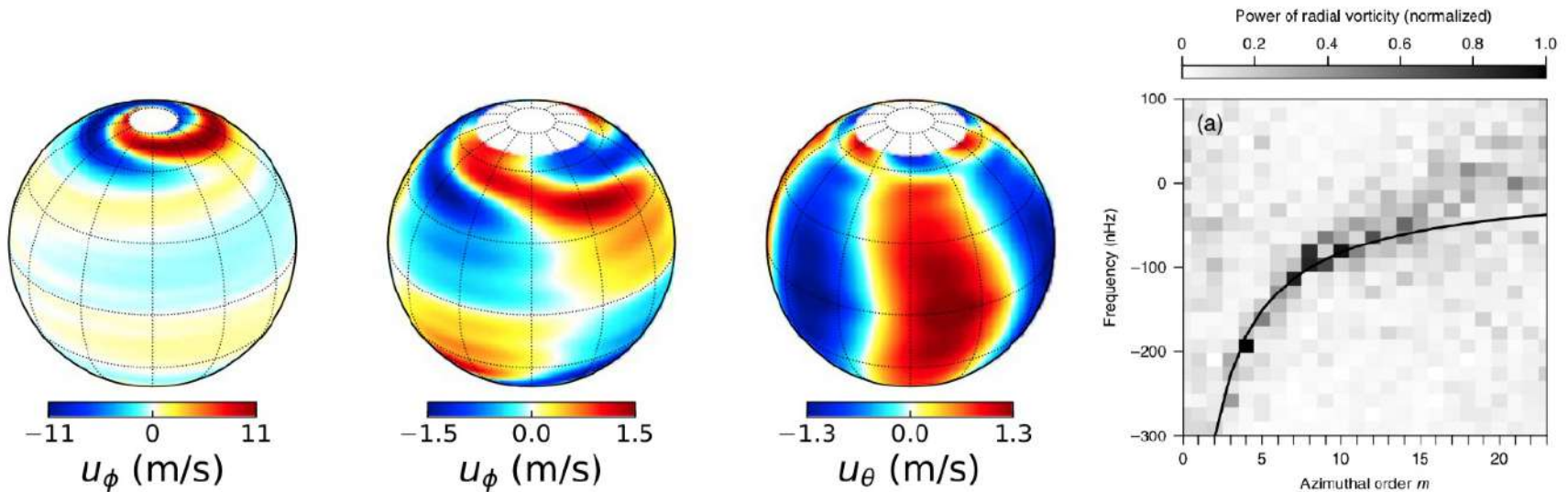


Figure 2.32 – From left to 2nd panel to the right we show: the $m = 1$ high-latitude spiral mode at -86 nHz, the $m = 2$ mid-latitude mode at -73 nHz (Gizon et al., 2021), the $m = 3$ equatorial (sectoral) Rossby mode at -269 nHz (Löptien et al., 2018a), adapted from (Gizon et al., 2024). Rightmost panel: Power spectrum of radial vorticity from local tracking of granulation, with the sectoral ($\ell = m$) Rossby mode dispersion relation ($\omega = -2\Omega_\odot/(m + 1)$) overplotted in black (Löptien et al., 2018a).

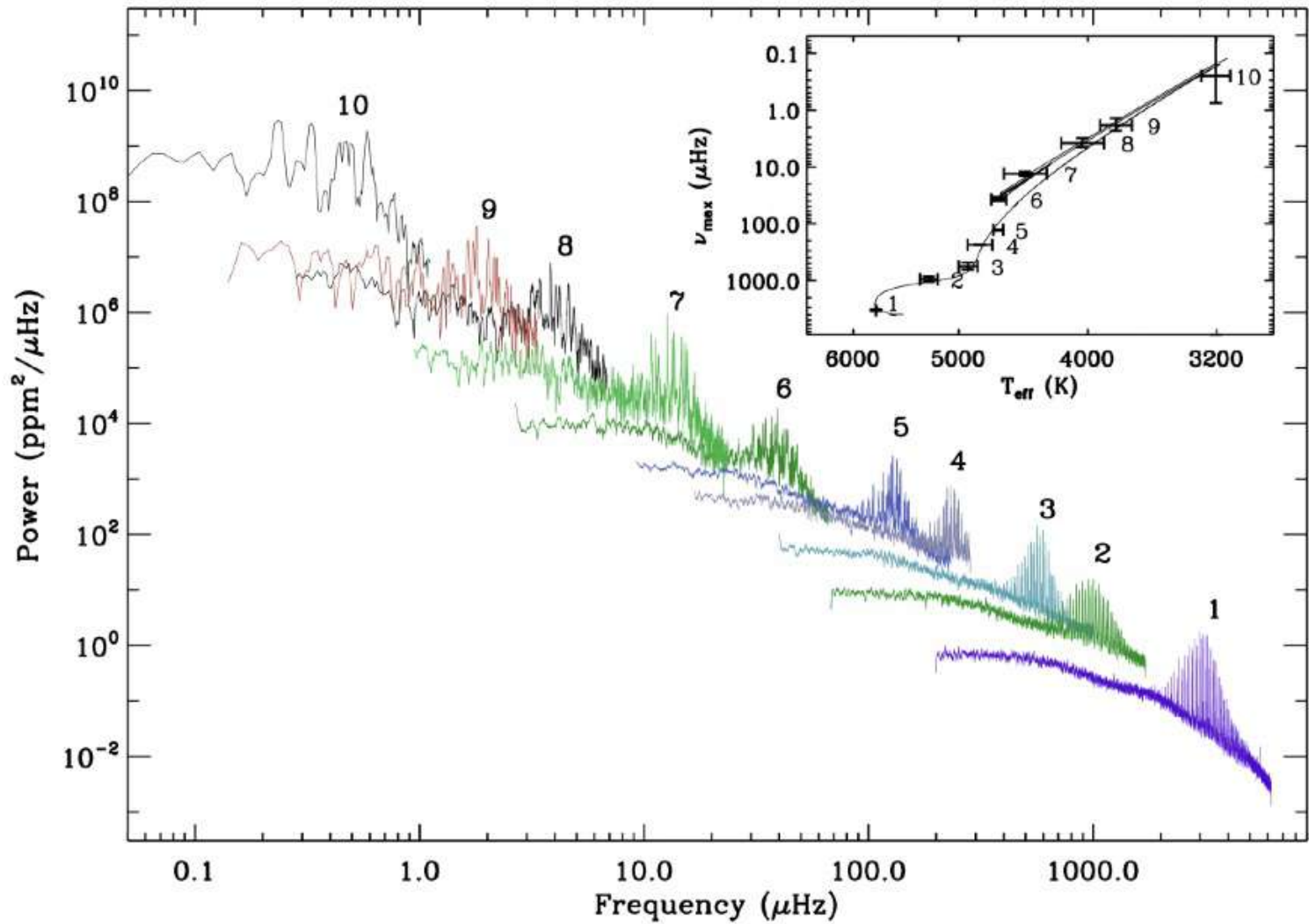
Gizon et al. 2021, see also Bekki et al. 2022

Basics of Asteroseismology

Allows to characterize internal structure and even core-envelope rotation contrast or internal magnetic fields

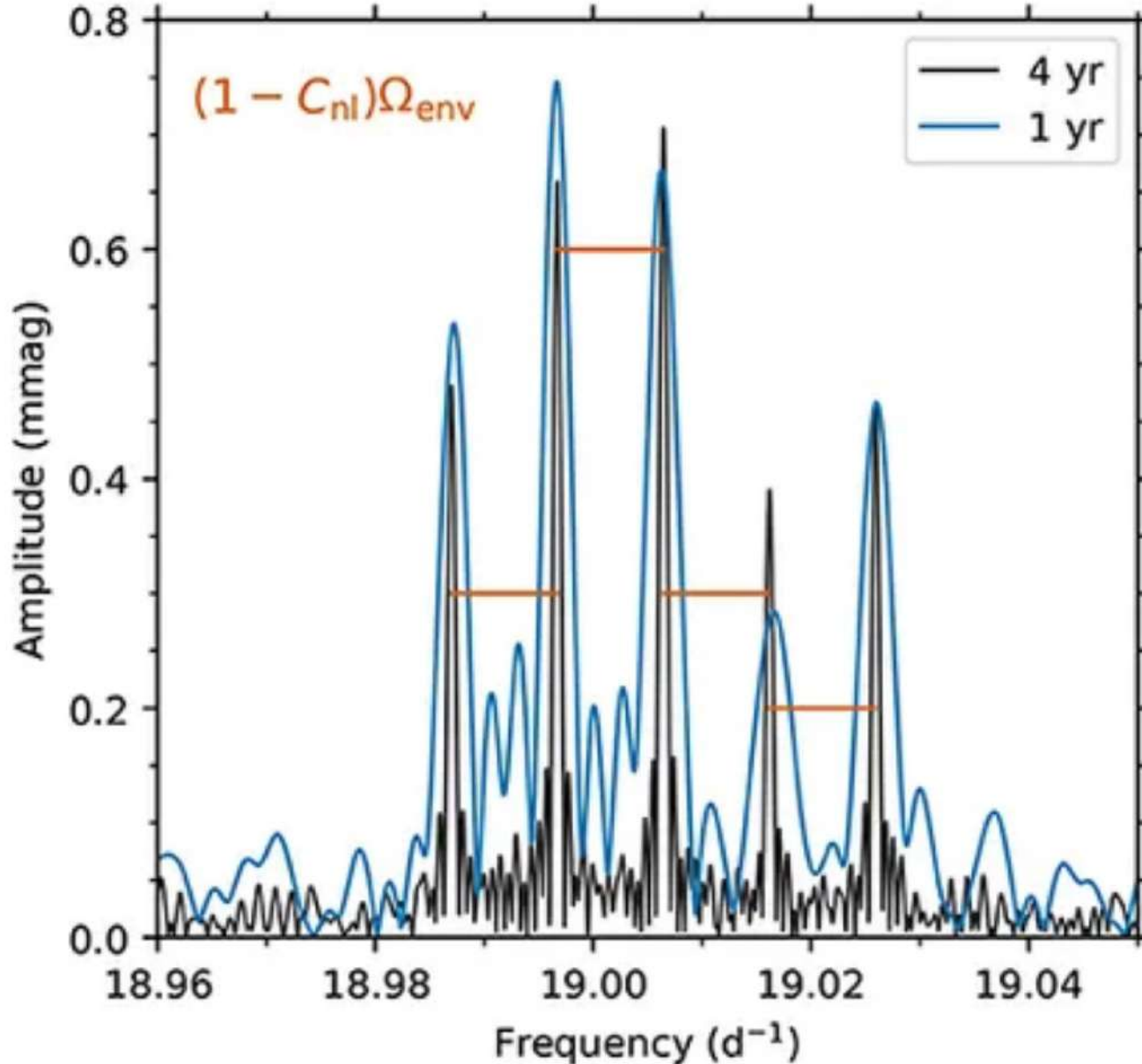
See Living Review by Ballot & Garcia 2018

Secular Evolution of ν_{\max}



Ballot & Garcia 2018 LRSP

Rotation Splitting in KIC 11145123



delta-scuti
star
~ 1.5 Msun
(late A/early F)
Very slow rotator

(Kurtz et al., 2014)

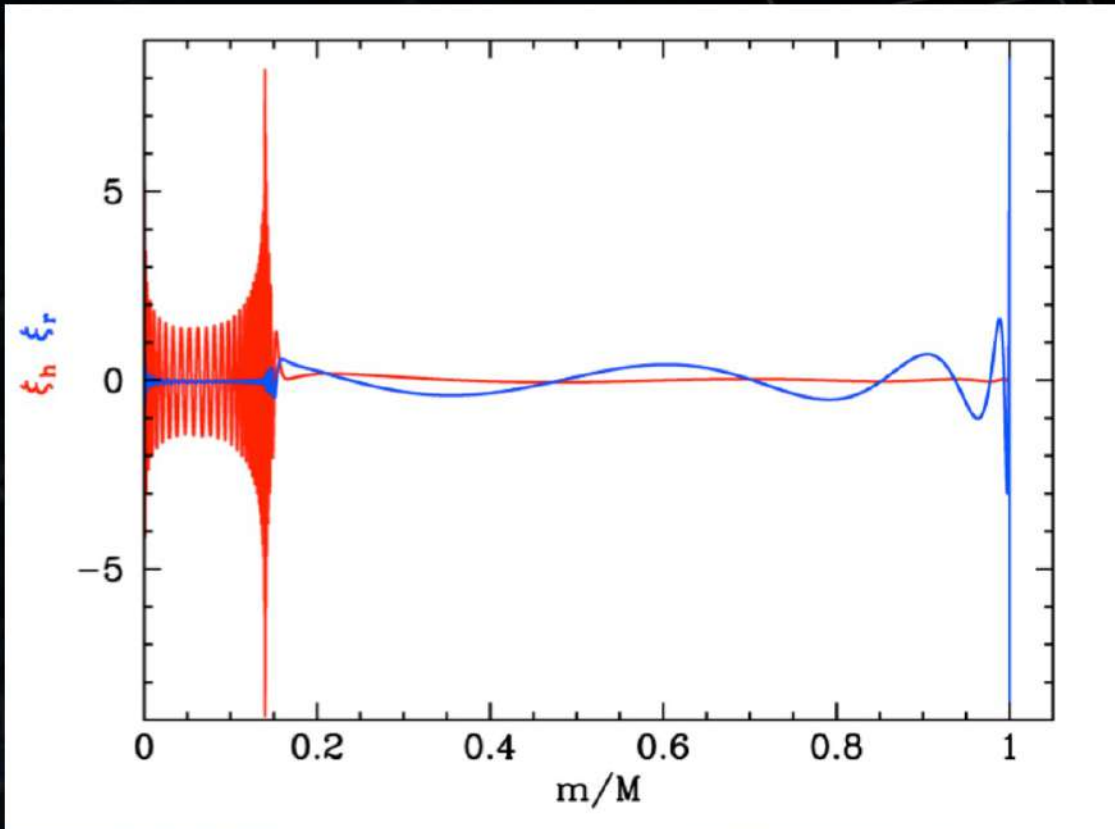
➤ **Mixed modes:**

- At the surface they behave as a p mode
- At the radiative internal region they behave as a g mode

➤ **Interest of mixed modes:**

- Sensitive to the core
- Much higher amplitudes than pure g modes

➤ **Strong constraints on the age of the stars**



[e.g. Metcalfe et al. 2010; Deheuvels et al. 2010]

Ensemble Asteroseismology and RGB rotation rate

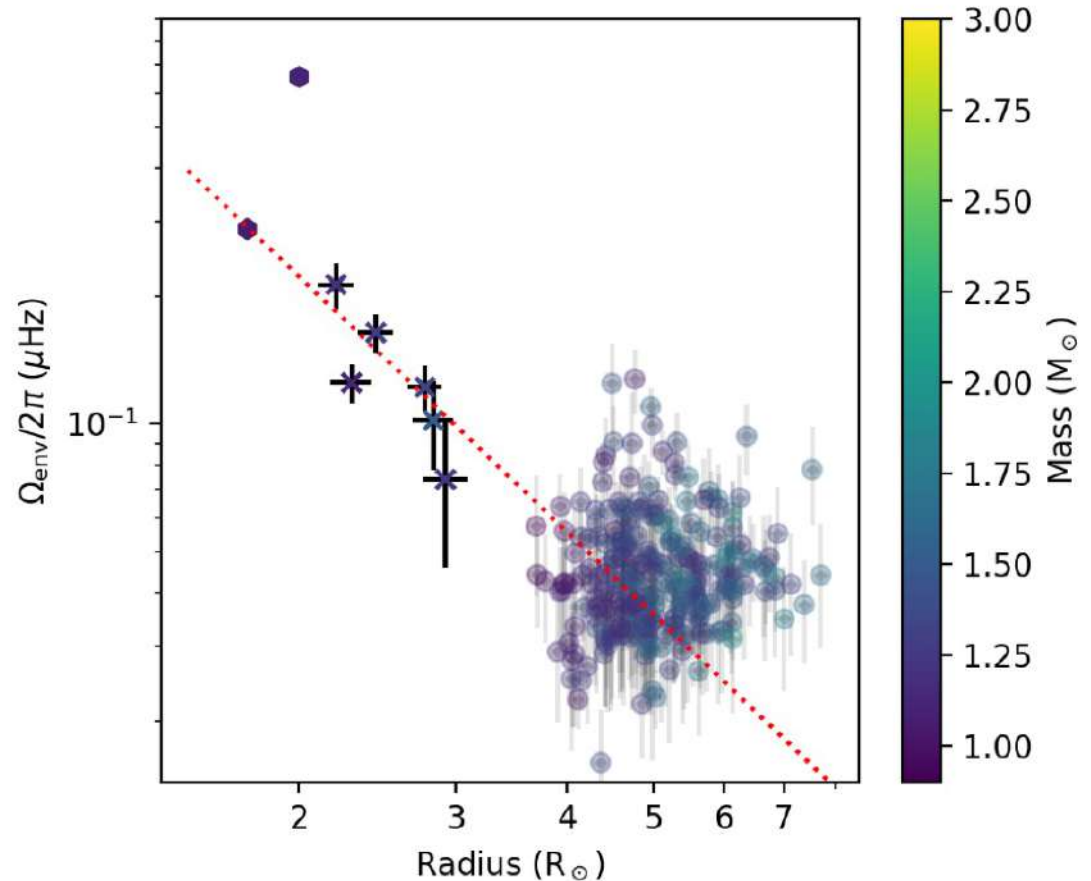
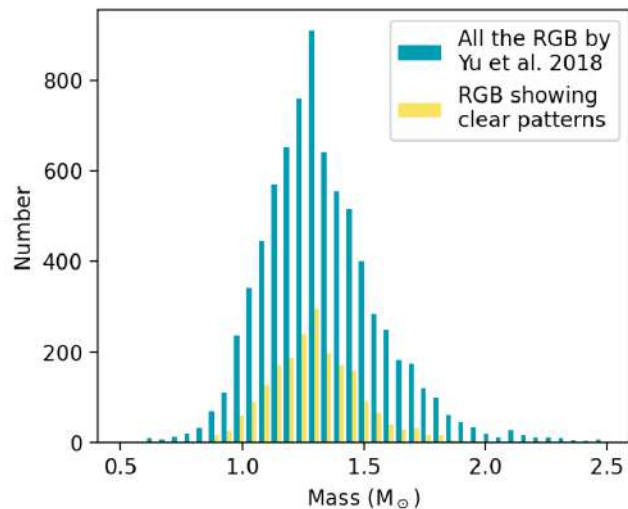
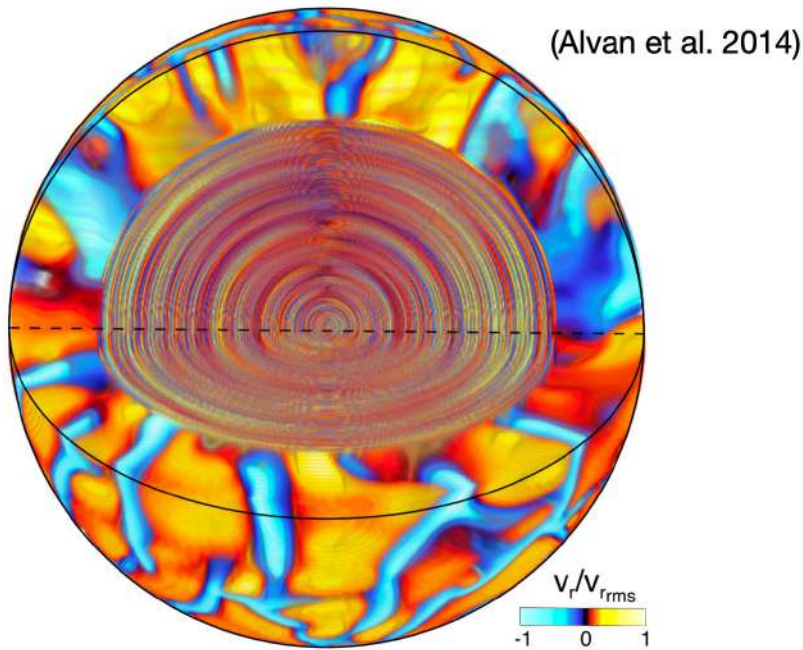


Fig. 12. Envelope rotation rate as a function of stellar radius. We include 243 RGB stars by this work whose envelope rotation rates are outside three sigma deviation from zero, six young RGB stars by [Deheuvels et al. \(2014\)](#), and two young RGB stars by [Deheuvels et al. \(2020\)](#). The red dotted line shows the best fitting results assuming the envelope rotation decreases with R^{-2} , which is $\Omega_p/2\pi = 0.97/R^2$.

3-D Numerical simulations of stellar oscillations

2 exemples: the Sun and an F-star

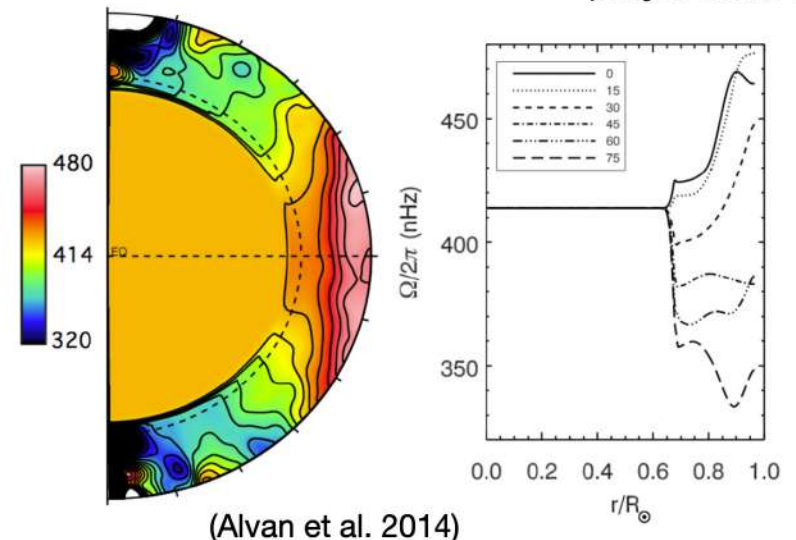
Modelling Gravity Waves in the Sun to Guide their Detection



Sun modelled from $r = 0$ to $0.97 R_{\odot}$

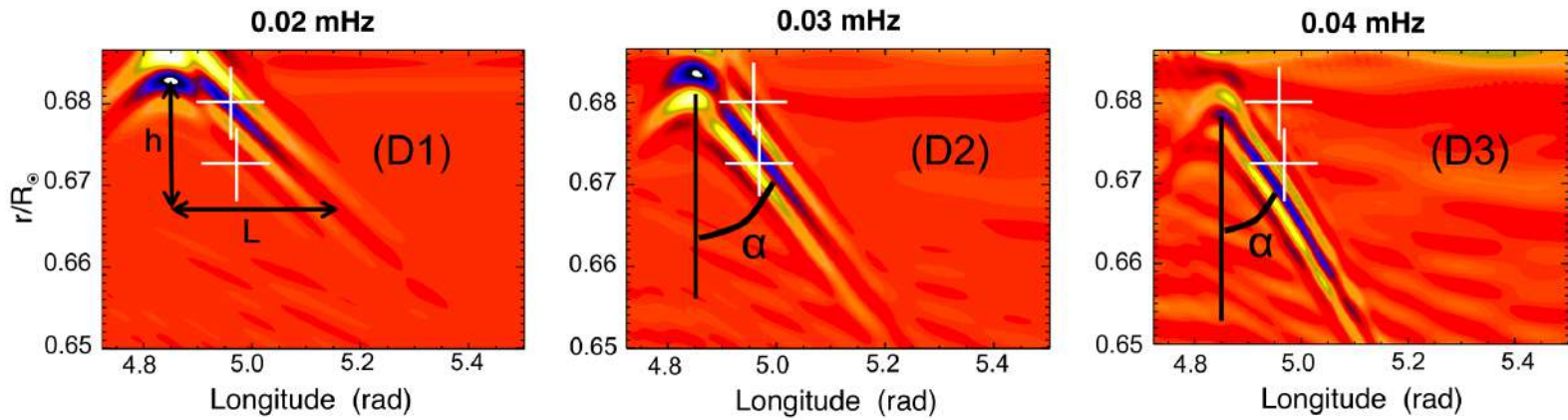
Coupling between convective and radiative zones:
gravity waves excitation by convective plumes

(Pinçon et al. 2016)

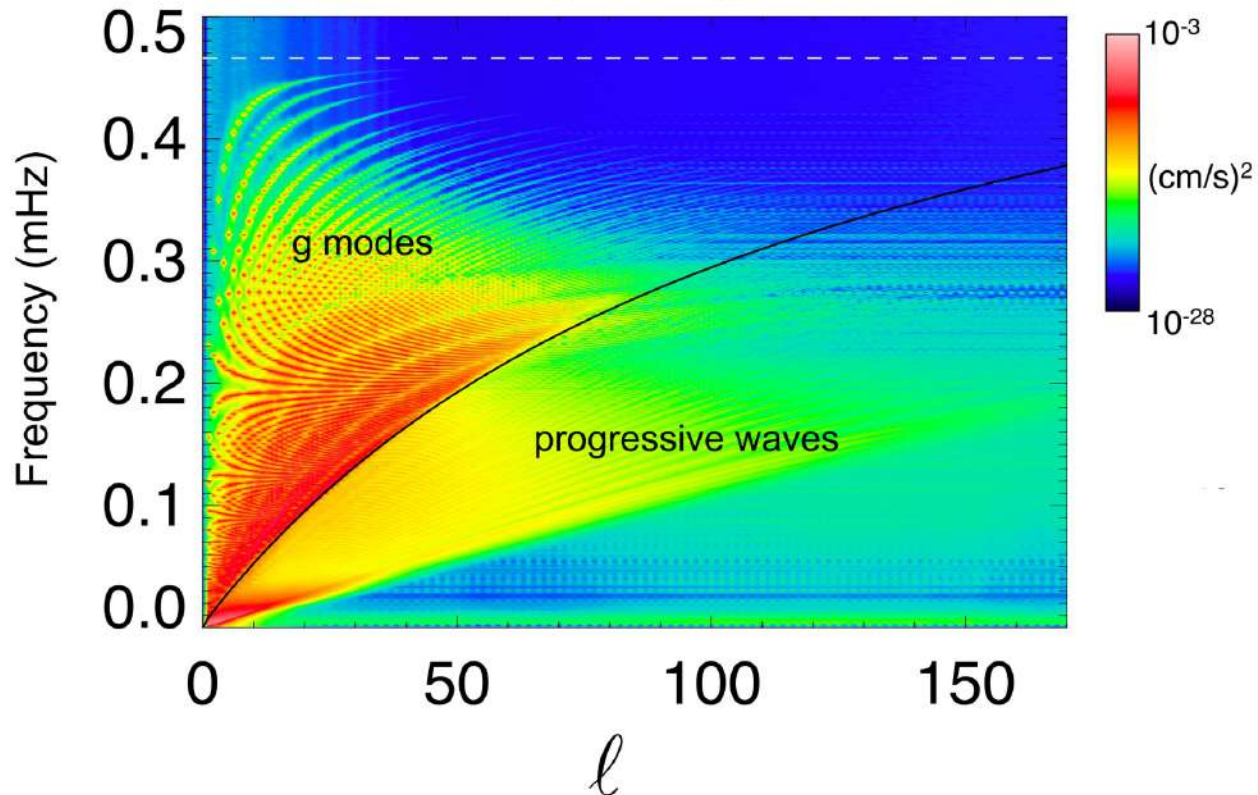


Need to extend the conclusions by
performing similar studies with F-type
stellar models

St-Andrews cross

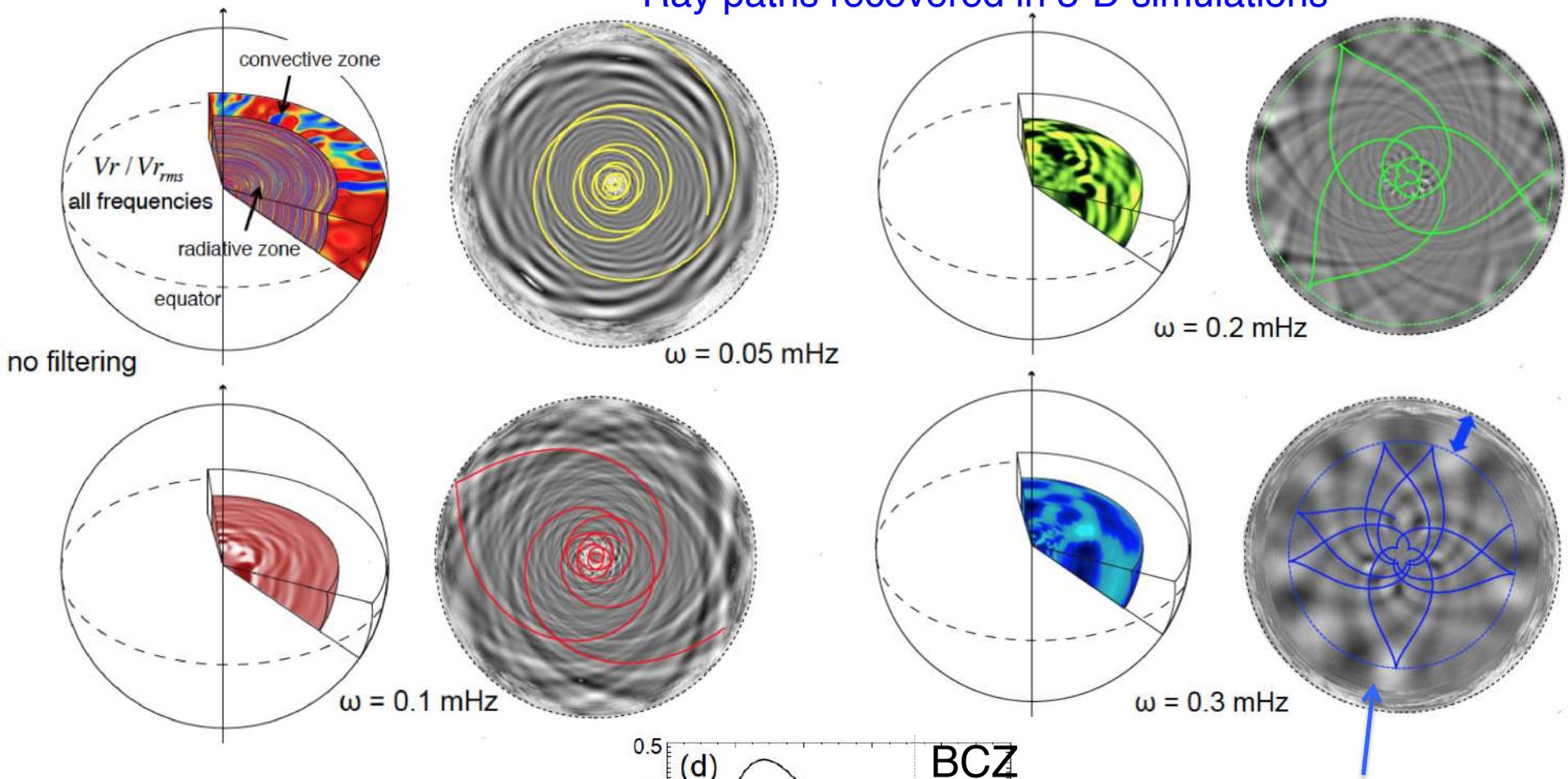


$$r_0 = 0.5R_{\odot}$$

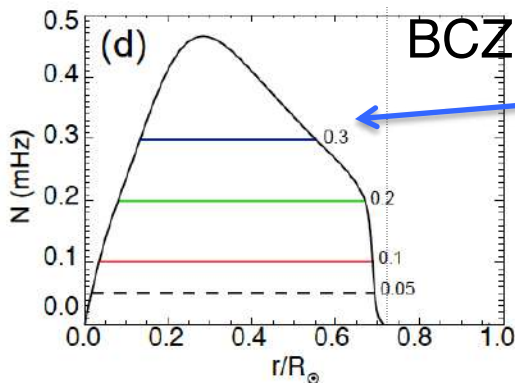


Internal Gravity Modes: Frequency Filtering

Ray paths recovered in 3-D simulations



Alvan, Brun et al. 2015

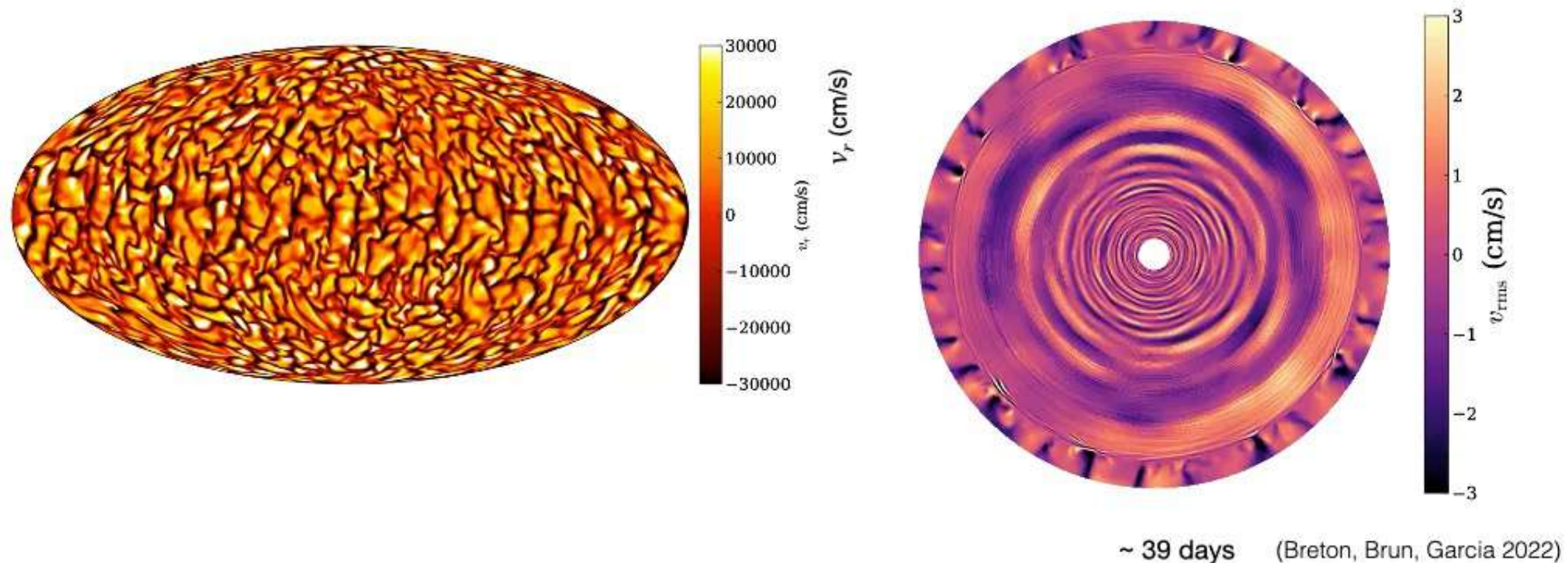


Note evanescent region

Convection and Gravity Waves in Fstars

Shallower convective envelope, g-modes could be easier to detect!

~ 39 days



For now omitting central core (see Breton, Brun, Garcia 2026, in press,
for a 2 Convection Zones Fstar 3-D simulation)

Next Lecture:

Solar corona, activity & heliosphere

